J. Braz. Chem. Soc., Vol. 8, No. 2, 143-147, 1997.
Printed in Brazil.

0103 – 5053 $6.00 + 0.00

Article

An Electrochemical Study of the Corrosion Processes of Ni-Based Glassy Metals in Aqueous Solutions

***M.R. Barbosa*[a]*, and *L.M. Gassa*[b]**

[a]*Facultad de Ingeniería, Universidad Nacional del Centro de la Provincia de Buenos Aires, C.C. 12, 7400 Olavarría, Argentina*

[b]*Instituto de Investigaciones Fisicoquímicas Teóricas y Aplicadas (INIFTA), Facultad de Ciencias Exactas, Universidad Nacional de La Plata, Sucursal 4, C.C. 16, 1900 La Plata, Argentina*

Received: June 30, 1996; January 20, 1997

O comportamento eletroquímico de ligas amorfas Ni-Co em soluções de carbonato/bicarbonato foi investigado usando espectroscopia de impedância eletroquímica combinada com voltametria e técnicas de polarização estacionárias. Os resultados indicam que a cinética do processo de dissolução é dependente do pH e da força iônica da solução eletrolítica. A composição do metal vítreo é um fator importante na determinação dos parâmetros cinéticos envolvidos no complexo comportamento eletroquímico desses materiais.

The electrochemical behavior of amorphous Ni-Co alloys in carbonate/bicarbonate solutions was investigated using electrochemical impedance spectroscopy combined with voltammetry and stationary polarization techniques. The results indicate that the kinetics of the dissolution processes are dependent on the pH and ionic strength of the electrolyte. The composition of the glassy metal is an important factor in determining the kinetic parameters involved in the complex electrochemical behavior of these materials.

Keywords: *impedance spectroscopy, glassy metals, Ni-Co alloys*

Introduction

Ni-Co amorphous alloys present an electrocatalytic activity on the OER in alkaline solution which is higher than that of their crystalline counterparts[1-8, and reference therein]. The use of these materials requires a satisfactory resistance to general and localized corrosion. It has been found[9] that the corrosion behavior of different polycrystalline Ni-Co alloys is a function of alloy composition.

A corrosion study of Ni-Co based glassy metals in carbonate-bicarbonate solutions at pH 8.9 showed that the dissolution processes are dependent on the ionic strength of the electrolyte[10].

The present study was undertaken in order to evaluate the influence of the pH and ionic strength of the electrolyte, as well as the alloy composition, on the corrosion behavior of a glassy Ni-based alloy (Vitrovac 0080), and to compare these results with Ni-Co based alloys.

Experimental

Amorphous alloys (Vakuumschmelze GmbH, Hanau) with the compositions Vitrovac 0080 ($Ni_{78}B_{14}Si_8$), G15 ($Ni_{58}Co_{20}B_{12}Si_{10}$) and G16($Ni_{25}Co_{50}B_{10}Si_{15}$), were employed as the working electrodes. A conventional three-compartment glass cell was used with a large area Pt counter electrode and a calomel reference electrode. Potentials in the text are referred to the normal hydrogen electrode (NHE) scale.

Electrochemical impedance spectroscopy (EIS) combined with steady-state current density/potential (j/E) curves, and single (STPS) and repetitive (RTPS) triangular potential sweeps, were performed under purified N_2 gas saturation in the following solutions: x M $KHCO_3$ + y M K_2CO_3 ($0.75 \leq x \leq 2.5$; $0.05 \leq y \leq 0.5$), covering the 8.3-10.5 pH range at 25 °C.

Results and Discussion

For the characterization of the electrochemical behavior of the amorphous alloys, voltammograms were run between the potential regions of the hydrogen and oxygen evolution reactions. The current density/potential (j/E) profiles corresponding to the first forward potential scan of G15 alloy in the different electrolyte solutions are presented in Fig. 1. The voltammetric profile in 0.05 M K_2CO_3 + 0.75 M $KHCO_3$ (pH 8.9) shows a first anodic current peak (Peak I) at *ca.* -0.3 V, associated with Ni/Ni(II) hydroxide transformation[11], a second anodic contribution (Peak II) at *ca.* 0.05 V, related to the oxidation of Co(II) to Co(III) oxides or hydroxides[12], and a third anodic current peak (Peak III) at *ca.* 0.7 V, associated with the redox couple Ni(II)/Ni(III)[11]. The current values of each peak are complex functions of the pH, ionic strength, and carbonate/bicarbonate ratio. j_{pI} increases and peak II appears less defined according to the ionic strength and pH. The influence of bicarbonate ions becomes evident at the top of peak III. The voltammograms of G16 (not shown here) also exhibit on the first anodic scan all of the current contributions described above. Furthermore, lower voltammetric charge densities of the peaks associated with Ni transformation are observed for G16 alloy in comparison with G15 alloy. It is interesting to note, that current peaks II related to the oxidation of Co(II) to Co(III) are the best defined, and that peak III appears at more negative potentials. This fact is associated with the increasing Co concentration in the alloy. This tendency is confirmed with data obtained under similar experimental conditions employing the non-Co containing alloy, Vitrovac 0080, in which case peak III shifts to 0.9 V. This Co effect has also been found by other authors[6,13].

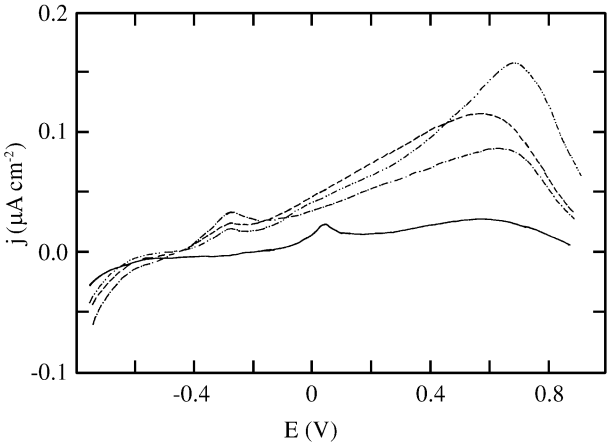

Figure 1. First forward going potential scan of the G15 alloy in different electrolyte solutions: (—) 0.05 M K_2CO_3 + 0.75 M $KHCO_3$ (pH = 8.9); (- - -) 0.17 M K_2CO_3 + 2.5 M $KHCO_3$ (pH = 8.9); (• - • -) 0.15 M K_2CO_3 + 0.75 M $KHCO_3$ (pH = 9.5) and; (•• - •• -) 0.5 M K_2CO_3 + 2.5 M $KHCO_3$ (pH = 9.5).

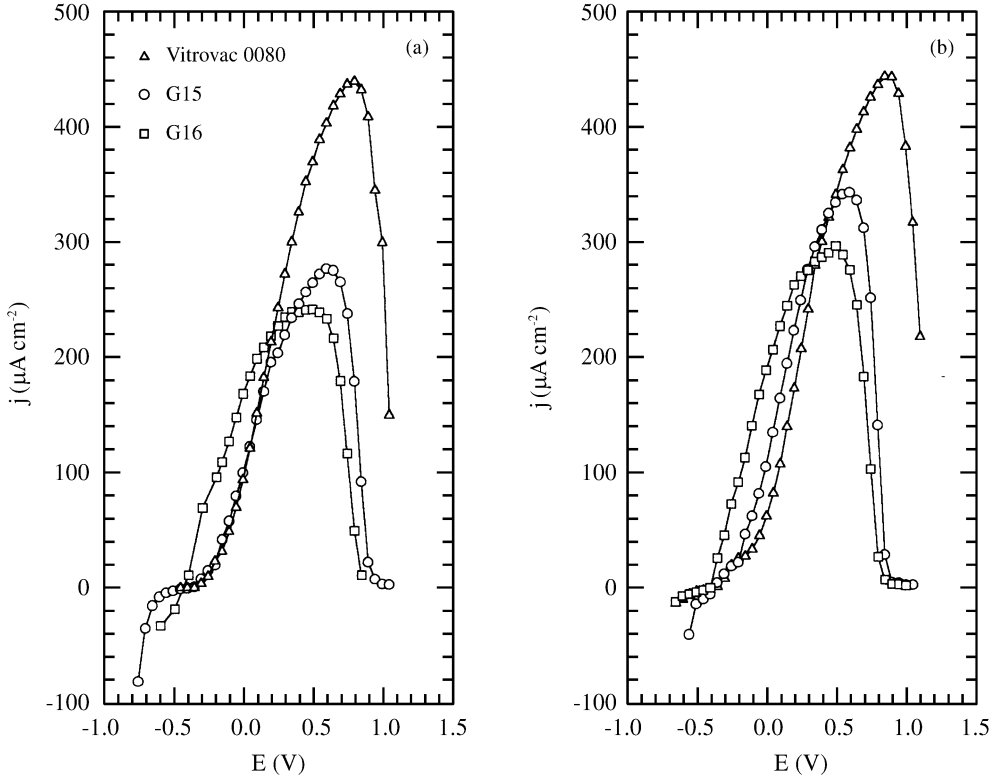

Figure 2. Stationary polarization curves of the Vitrovac 0080, G15, and G16 alloys in (a)0.167 M K_2CO_3 + 2.5 M $KHCO_3$ (pH 8.9) and (b) 0.5 M K_2CO_3 + 2.5 M $KHCO_3$ (pH = 9.5) solutions.

The steady state polarization curves of Vitrovac 0080, G15, and G16 electrodes in 0.167 M K_2CO_3 + 2.5 M $KHCO_3$ (pH 8.9) and 0.5 M K_2CO_3 + 2.5 M $KHCO_3$ (pH = 9.5) are shown in Figs. 2a and 2b, where the dots indicate the potentials at which impedance spectra were recorded.

The current contribution at about 0.6 V can be associated with the redox couple Ni(II)/Ni(III)[11]. It is worth noting that this current peak appears at more positive potentials for the non Co-containing alloy. This effect was also found by Lian *et al.*[6], who suggested that cobalt additions to $Ni(OH)_2$ stabilize Ni hydroxide, improve the conductivity and charge efficiency of $Ni(OH)_2$, and increase the oxygen overpotential. Furthermore, Folquer *et al.*[13] found a catalytic effect of the Co(II)/Co(III) reaction on the Ni(II)/Ni(III) reaction in co-precipitated Ni-Co alloys through hydroxide ions inserted into the metal hydroxide layers.

At a constant pH, the high value of the current peak (j_p) increases with increasing Ni concentration in the alloys and the ionic strength of the electrolyte. These effects hold for all of the tested alloys. On the other hand, as pH increases (Fig. 2b) the value of the j_p becomes higher for the Co-containing alloy and remains practically constant in the case of Vitrovac 0080. At a constant concentration of bicarbonate ions, linear log j_p *vs.* pH relationships are obtained with a slope of 0.42 ± 0.05 for G15 and 0.4 ± 0.02 for G16. Accordingly, the data revealed a complex effect of carbonate/bicarbonate ions on the corrosion behavior of Ni-Co based glassy metals.

The frequency response of each investigated amorphous alloy was found to be remarkably dependent on the applied potential, on the alloy composition, and on the electrolyte concentration. Nyquist plots recorded with Vitrovac 0080 in 0.167 M K_2CO_3 + 2.5 M $KHCO_3$ (Fig. 3) exhibit a capacitive semicircle at potential values close to the corrosion potential (Fig. 3a), and at more positive polarizations an inductive contribution appears at the intermediate frequencies, where a new time constant at low frequencies can be observed (Figs. 3b-e). As the anodic polarization increases, the resistance values associated with the low frequency contribution become negative (Fig. 3f). The above-described influence of the electrolyte composition on the steady-state measurement is also observed in the impedance data.

Otherwise, the impedance response obtained in the case of the Co-containing alloys (G15 and G16) in carbonate/bicarbonate solutions presents the same general features as the Vitrovac 0080 one, but involves higher inductance, which in turn hinders the appearance of a well-defined inductive behavior at intermediate frequencies and a non-complete capacitive semicircle at low frequencies (see, for instance, Figs. 4 and 5). The higher impedance values obtained employing these alloys in comparison with Vitrovac 0080 are consistent with the lower current densities under steady-state conditions for the alloy with a higher Co content.

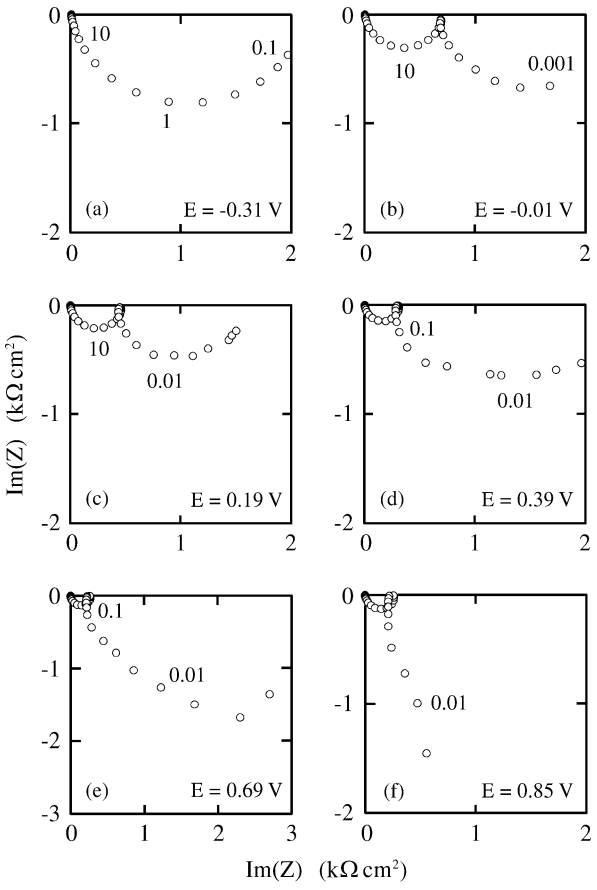

Figure 3. Nyquist diagrams of alloy Vitrovac 0080 at different applied potentials. Solution 0.167 M K_2CO_3 + 2.5 M $KHCO_3$ (pH 8.9).

The whole set of experimental impedance spectra can be discussed according to the following total transfer function:

$$Z_T(j\omega) = R_\Omega + Z \quad (1)$$

with

$$Z^{-1} = [CPE]^{-1} + [R_{ct} + \frac{j\omega L R_{ic}}{j\omega L + R_{ic}} + \frac{R_{ad}}{j\omega C_{ad} R_{ad} + 1}]^{-1} \quad (2)$$

where R^Ω is the electrolyte resistance contribution, $\omega = 2\pi f$, [CPE] denotes the constant phase element given by $[CPE] = [C_{dl}(j\omega)^\alpha]^{-1}$, C_{dl} is the Helmholtz layer capacitance, α takes into account the distribution of time con-

stants due to surface unhomogeneities in the amorphous alloys, R_{ct} represents the charge transfer resistance defined as $Z(\omega = \infty)$, L and R_{ic} are associated with the inductive

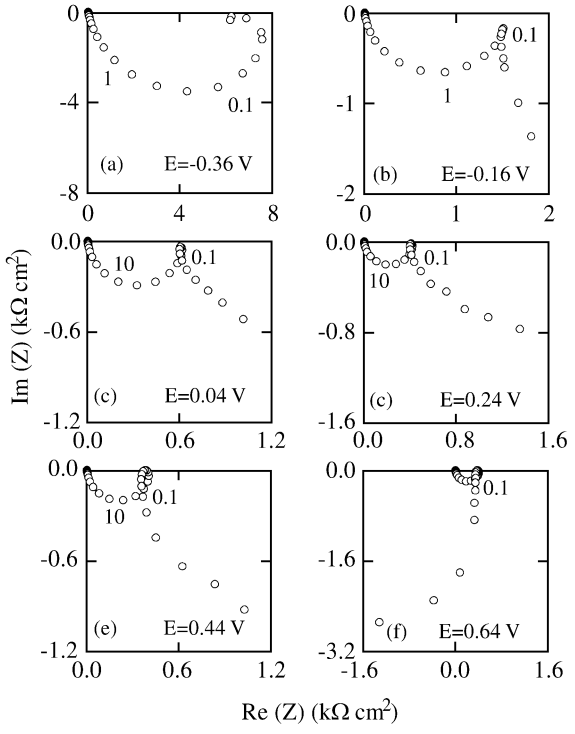

Figure 4. Nyquist diagrams of the G15 alloy at different applied potentials. Solution 0.167 M K_2CO_3 + 2.5 M $KHCO_3$ (pH 8.9).

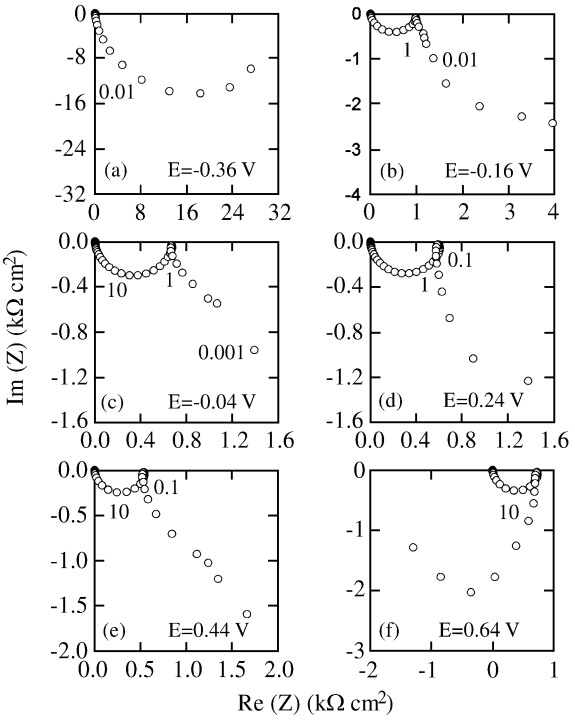

Figure 5. Nyquist diagrams of the G16 alloy at different applied potentials. Solution 0.167 M K_2CO_3 + 2.5 M $KHCO_3$ (pH 8.9).

contribution which can be interpreted by assuming a strong potential dependence of the active site concentration causing surface relaxation phenomena, and R_{ad} and C_{ad} can be related, in principle, to a Faradaic pseudo-capacitive contribution of an adsorbed reaction intermediate at the lowest frequencies.

The good agreement between the experimental and simulated data according to transfer function (1) analysis using non-linear least-square fit routines is demonstrated in Figs. 6 and 7 in 0.167 M K_2CO_3 + 2.5 M $KHCO_3$ (pH = 8.9) and 0.5 M K_2CO_3 + 2.5 M $KHCO_3$ (pH = 9.5) solutions, respectively.

The values of C_{dl} and R_{ct} were determined from the optimum fitting according to Eq. 1. In the potential range -0.4 V≤ E ≤ 0 V, it was possible to estimate mean values by C_{dl} = 30 ± 10 μF cm^{-2} and α = 0.95 ± 0.05, while the value of R_{ct} decreases linearly. At positive applied potentials the R_{ct} values are nearly constant and lower capacitance values, C = 9 ± 2 μF cm^{-2}, are obtained. These low C values are typical of a metal covered with a passive film[14], and may be considered the passive film and double layer capacitance connected in series. The potential independence of the capacitance indicates either insulating or semiconducting properties of the passive films. At E ± 0 V, $R_{ct} = 0.434\ b/j_{ss}$ for a charge transfer controlled reaction, where j_{ss} denotes the steady-state current density and $b = \partial E/\partial \log|j_{ss}|$ I is the

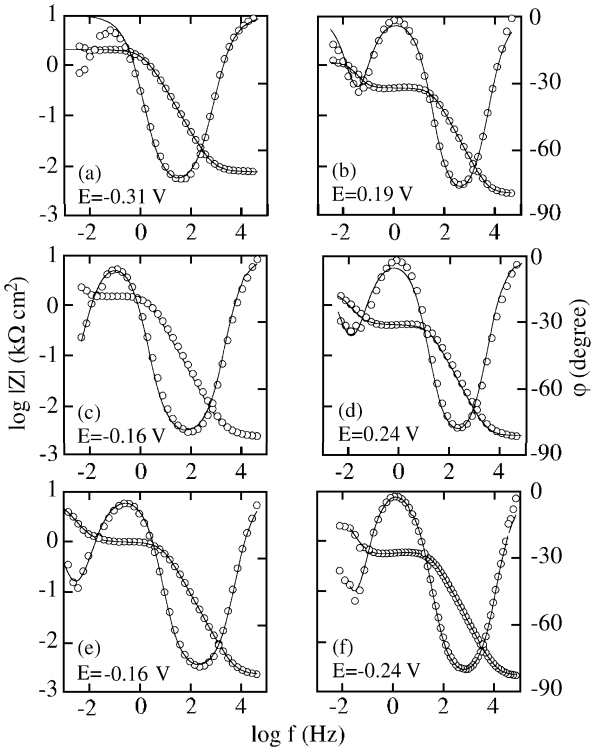

Figure 6. Comparison of the experimental (o) and fitted (-) Bode plots of the a,b) Vitrovac 0080, c,d) G15, and e,f) G16 alloys in 0.167 M K_2CO_3 + 2.5 M $KHCO_3$ (pH 8.9).

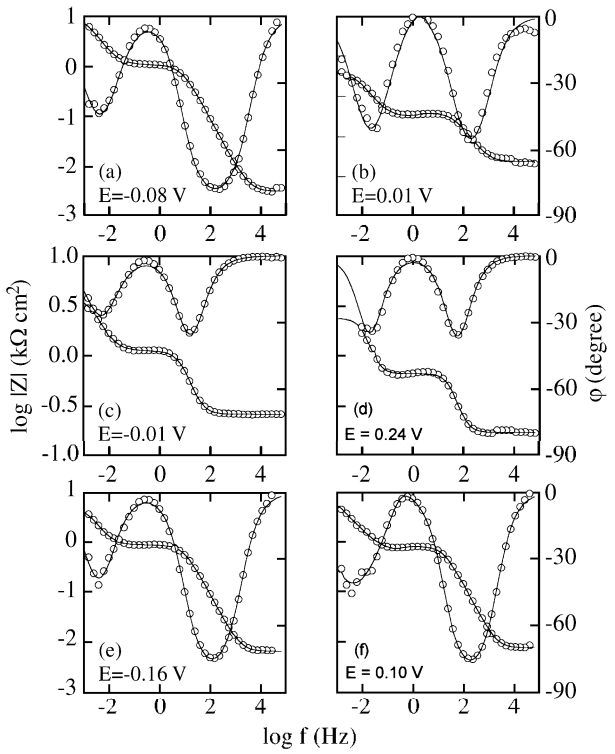

Figure 7. Comparison of the experimental (o) and fitted (-) Bode plots of the a,b) Vitrovac 0080, c,d) G15, and e,f) G16 alloys in 0.5 M K_2CO_3 + 2.5 M $KHCO_3$ (pH = 9.5).

Tafel slope of the anodic reaction, b ≈ 120 mV was found, corresponding to a charge transfer coefficient of 0.5.

The analysis of the impedance parameters associated with the time constant contribution at the lowest frequencies is difficult in the case of alloys G15 and G16 due to an incomplete capacitive profile, although it was possible to estimate a value of $C_{ad} \approx 860 \pm 60\ \mu F/cm^2$. The values of resistance and capacitance associated with the second capacitive loop for Vitrovac 0080 were close to $3.5 \pm 0.2\ k\Omega\ cm^2$ and 4 ± 0.2 mF/cm^2, respectively.

It is possible to conclude, in principle, that the fit parameters related to the inductive loop observed at intermediate frequencies fail to obey a direct function of the Ni/Co concentration ratio in the alloy matrix. This fact is reaffirmed by the experimental results obtained with Vitrovac 0080, which present a clear inductive contribution at intermediate frequencies.

The impedance results clearly show that the dissolution processes are taking place through a complex reaction mechanism, and it is necessary to determine the composition of the surface films formed on amorphous alloys under different polarization conditions. Consequently, XPS studies are in progress.

Acknowledgments

This research project was financially supported by the Consejo Nacional de Investigaciones Científicas y Técnicas, the Comision de Investigaciones de la Provincia de Buenos Aires, and the Fundación Antorchas. Part of the equipment used in the present work was provided by DAAD and the Alexander von Humboldt-Stiftung.

References

1. Kreysa, G.; Hakansson, B. *J. Electroanal. Chem.* **1986**, *201*, 61.
2. Alemu, H.; Jüttner, K. *Electrochim. Acta* **1988**, *33*, 1011.
3. Kessler, T.; Vilche, J.R.; Ebert, M.; Jüttner, K.; Lorenz, W.J. *Chem. Eng. Technol.* **1991**, *14*, 263.
4. Lian, K.; Kirk, D.W.; Thorpe, S.J. *Electrochim. Acta* **1991**, *36*, 537.
5. Lian, K.; Thorpe, S.J.; Kirk, D.W. *Electrochim. Acta* **1992**, *37*, 169.
6. Lian, K.; Thorpe, S.J.; Kirk, D.W. *Electrochim. Acta* **1992**, *37*, 2029.
7. Kupka, J.; Budniok, A. *J. Appl. Electrochem.* **1990**, *20*, 1015.
8. Lian, K.; Kirk, D.W.; Thorpe, S.J. *J. Electrochem. Soc.* **1995**, *142*, 3704.
9. Ball, G.R.; Payer, J.H. In *Proc. 12th. International Corrosion Congress*; Houston, 1993, 1132.
10. Gassa, L.M.; Vilche, J.R.; Barbosa, M.R. *Materials Science. Forum* **1995**, *192-194*, 825.
11. Bohé, A.E.; Vilche, J.R.; Arvia, A.J. *J. Appl. Electrochem.* **1990**, *20*, 418.
12. Gervasi, C.A.; Biaggio, S.R.; Vilche, J.R.; Arvia, A.J. *Corros. Sci.* **1989**, *29*, 427.
13. Folquer, M.E.; Vilche, J.R.; Arvia, A.J. *J. Electroanal. Chem.* **1984**, *172*, 235.
14. Simões, A.M.P.; Ferreira, M.G.S.; Rondot, B.; da Cunha Belo, M. *J. Electrochem. Soc.* **1990**, *137*, 82.